

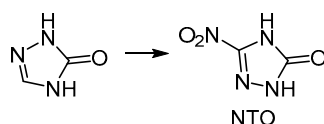
3-Nitro-1,2,4-triazol-5-one (NTO): high explosive insensitive energetic material

Ruksana R. Sirach¹, Pragnesh N. Dave^{1*}

¹ Department of Chemistry, Sardar Patel University,
Vallabh Vidyanagar, 388120, Gujarat, India; e-mail: pragnesh7@yahoo.com

Published in Khimiya Geterotsiklicheskih Soedinenii,
2021, 57(7/8), 720–730

Submitted May 12, 2021
Accepted after revision July 6, 2021



- Less sensitive
- Synthesized in laboratory conditions
- Morphology and polymorphism steered by crystallization solvent system
- Thermal decomposition temperature decreased by smaller particle size
- Thermal decomposition temperature steered by catalyst

5-Nitro-3*H*-1,2,4-triazol-3-one (NTO) also known as nitrotriazolone is a low sensitive and thermally stable high energetic material containing a heterocyclic ring. NTO can be used to substitute highly sensitive high energetic materials that are thermally and photochemically less stable. This review provides a survey of various routes utilized for the synthesis of NTO, changes in its morphology by varying solvent systems, characterization, decomposition mechanisms, and use of metal oxides and other catalysts to enhance or diminish the thermal decomposition temperature of NTO. The review covers research on the synthesis, thermal decomposition mechanism, and catalytic effect of NTO additives from past four decades (1987–2021).

Keywords: 5-nitro-3*H*-1,2,4-triazol-3-one (NTO), nitrotriazolone, decomposition mechanism, morphology, synthesis.

For a long time high energetic materials (HEMs) are known to be used both for civilian and military purposes.^{1,2} These energetic materials find applications as low explosives (propellants and pyrotechnics) and high explosives.³ Research has been carried out to enhance the thermal stability, burn rate, insensitivity to external force, and to synthesize new energetic materials with enhanced properties.² Nanomaterials can be used to enhance thermal decomposition of energetic materials and consequently improve their performance.⁴ A great deal of research has been carried out to enhance the performance of these energetic materials by adding catalysts, modifying the existing energetic materials to increase their performance, creating so-called cocrystals or by synthesizing new energetic materials.^{5–18}

Organic compounds that are mainly used as high energetic materials are rich in nitrogen content and more often than not contain nitro, azide, and/or hydrazino groups in their structure.^{6–9,11,15–19} 1,3,5,7-Tetranitro-1,3,5,7-tetrazocane (HMX, octogen), 1,3,5-trinitroperhydro-1,3,5-triazine (RDX), and trinitrotoluene (TNT) are some of the conventional nitrogen-containing high explosive organic compounds, but these explosives are highly sensitive, as they detonate rapidly under external forces like friction, heat, spark, etc. Therefore, it is desirable to produce high-performance energetic materials (EMs) with excellent

combustion/detonation properties, high density, and positive oxygen balance, as well as good thermal stability, insensitivity to external force, characterized by economical synthesis, safe handling, and good environmental compatibility.^{5,20}

To overcome these problems, a less sensitive heterocyclic high energetic material 5-nitro-2,4-dihydro-3*H*-1,2,4-triazol-3-one (NTO) is being investigated as a possible replacement of the popular explosives mentioned above.^{2,21} Thus, a series of insensitive munitions explosive (IMX) compositions containing 2,4-dinitroanisole (DNAN) as a melt-cast binding agent, NTO, and RDX were used for preparing less sensitive explosives with enhanced performance.²² These compositions are expected to become more popular as the need for insensitive weapons grows.²³ The term NTO is also used in literature for nitro group containing triazolones: 5-nitro-1,2,4-triazol-3-one or 3-nitro-1,2,4-triazol-5-one and its various hydrogenated forms in which ring is partially reduced (5-nitro-2,4-dihydro-3*H*-1,2,4-triazol-3-one (alternatively called 3-nitro-1*H*-1,2,4-triazol-5(4*H*)-one), 5-nitro-4,5-dihydro-3*H*-1,2,4-triazol-3-one, or 5-nitro-1,2-dihydro-3*H*-1,2,4-triazol-3-one) or completely reduced (5-nitro-1,2,4-triazolidin-3-one).^{2,21} In the present review, the abbreviation NTO is mainly used for 5-nitro-2,4-dihydro-3*H*-1,2,4-triazol-3-one, which is also referred in literature by its general name 3-nitro-1,2,4-triazol-5-one.

NTO has certain limitations such as acidic nature, negative enthalpy, increased explosive sensitivity in the presence of moisture,²⁴ and negative oxygen balance that restricts its applications.² In addition to that, NTO is water-soluble (>2 g/l), has poor adsorption affinity in clay soils, limited adsorption affinity for organic materials from natural sources such as plants and animals and is resistant to degradation in oxic soils. Hence, soil contamination resulting from incomplete detonations has the potential to contaminate ground water as well as possible environmental effect and toxic effect upon human exposures.²⁵ To overcome these problems, various studies have been carried out to improve the detection and degradation of NTO in the soil and wastewater.^{26–28}

NTO can be used as an additive to other high energetic materials to improve their performance, or further derivatization of NTO can be done to improve its performance. Zhang et al. prepared numerous salts of NTO by replacing the acidic proton attached to the nitrogen atom with several cations and obtained products with thermal decomposition temperatures in the range of 203–270°C, which is comparable to that of RDX (230°C), 1,3,5-triamino-2,4,6-trinitrobenzene (TATB) (330°C), and hexanitrohexaazaisowurtzitane-CL-20 (210°C).²⁹ Yang and Fude concluded that when NTO is added to HMX, the resulting core/shell structured composite HMX/NTO particles have lower frictional and impact sensitivity compared to HMX alone.³⁰ In a similar way, the partial replacement of RDX with NTO in explosive formulations based on hydroxyl-terminated polybutadiene (HTPB) provided a better shock sensitivity than that of RDX alone.³¹ Many analytical techniques have been employed in the past to understand the decomposition mechanisms of energetic materials, such as thermogravimetry coupled with mass spectroscopy (TG-MS) or Fourier transform infrared spectroscopy (TG-FTIR) to name a few.³² This review provides a brief overview of synthesis, properties, morphology, and decomposition mechanisms of NTO.

1. SYNTHESIS OF NTO

Manchot and Noll are considered the pioneers in synthesizing NTO,³³ but the structure assigned by them was incorrect. Thereafter, Chipen et al. have synthesized 1,2,4-triazol-5-one and its derivatives.³⁴ Later, Lee et al. successfully synthesized NTO and reported on its explosive nature.²⁰ Substantial efforts have been undertaken to synthesize NTO using conventional methods,^{20,34–36} a microwave-assisted method,³⁷ using several nitrating agents with varying concentrations,^{38–40} varying the ratio of reagents,³⁶ changing the morphology of the produced NTO by varying the recrystallization solvent,⁴¹ exploring the effect of ultrasound on the recrystallization,⁴² reducing the size of the synthesized NTO particles,⁴³ nanosizing of NTO,^{44,45} and obtaining NTO in form of metal salts.^{34,46} The most common method used for the synthesis of NTO involves 2 steps: (1) synthesis of 1,2,4-triazol-5-one (1), (2) nitration of compound 1 to NTO using various nitrating agents. The structures of compound 1 (shown as 1*H*-1,2,4-triazol-5-one tautomer) and NTO are depicted in Figure 1.

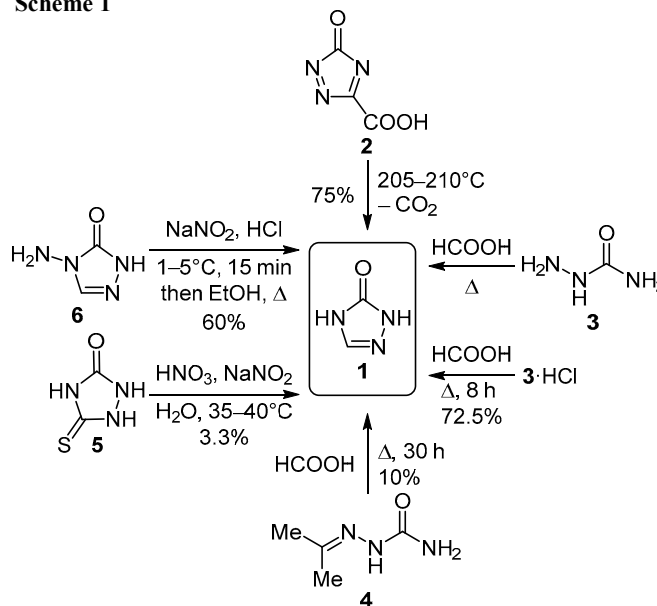


Figure 1. Chemical structures of 1,2,4-triazol-5-one (1) and NTO.³⁴

1.1. Synthesis of 1,2,4-triazol-5-one

A substantial body of literature is available on synthesizing 1,2,4-triazol-5-one (1) employing various methods (Scheme 1). One of them is carboxylation of 3-oxo-3*H*-1,2,4-triazole-5-carboxylic acid (2).^{34,47} Thus, Chipen et al. obtained compound 1 in 75% yield by decarboxylating 3-oxo-3*H*-1,2,4-triazole-5-carboxylic acid (2) at 205–210°C.³⁴ Another group of methods involves cyclocondensation by refluxing formic acid with semicarbazide (3)³⁶ or its hydrochloride^{20,34,35,42} or acetone semicarbazone (4)³⁴ in various molar ratios. Formic acid initially dissolves substrate 2–4 producing a homogeneous mixture which upon removing the excess formic acid yields compound 1 as a white solid mass.^{20,34–36,42}

Scheme 1



A widely employed protocol involves heating of semicarbazide hydrochloride (3·HCl) with HCOOH under reflux followed by distilling off the excess of HCOOH, followed by the addition of H₂O and evaporating to dryness and recrystallization from EtOH or H₂O. Thus Chipen et al. synthesized compound 1 by refluxing semicarbazide hydrochloride (3·HCl) with excess of HCOOH until it dissolved. By removing the excess of HCOOH the solid product was obtained with a 72.5% yield.³⁴ Russian scientists Starodubova et al.,⁴⁸ optimized the reaction time and the temperature conditions for the synthesis of 1,2,4-triazol-5-one (1) using semicarbazide hydrochloride (3·HCl) and formic acid. It was observed that time (0.05–5 h) and temperature (85–90, 102–104, and 110–112°C) variation causes changes in the product yields to vary in the range 5–67%. The best yield (67.16 %, reaction time 3 h) of

compound **1** with a better rate constant (22.9×10^2 mol/s) was obtained at the temperature range of 110–112°C as compared to that at the temperature range 85–90°C (4.97×10^2 mol/s, 42.47% yield, 5 h) and 102–104°C (8.87×10^2 mol/s, 55.86%, 3 h). The reaction yield and the reaction rate thus increases with increasing the temperature ranges of the reaction.⁴⁸ In this method, the highly toxic and corrosive HCl gas is released. To overcome this problem, semicarbazide free base **3** is used. It is synthesized by heating a mixture of hydrazine hydrate and urea at 100°C for 4 h and allowing the mixture to stand overnight in alcoholic conditions followed by cooling and recrystallization of semicarbazide (**3**) from alcohol yielding a white solid. Refluxing semicarbazide (**3**) with excess of HCOOH yields product **1**. The molar ratio of compound **3** to HCOOH was varied from 1:1 to 1:10 and the best results were obtained when this ratio was 1:4.³⁶ Compound **1** thus obtained was recrystallized using various solvents (Me₂CO, EtOH, H₂O, etc., mp 234°C) or used without recrystallization for further nitration.²⁰

Chipen et al. refluxed acetone semicarbazone (**4**) with excess of HCOOH for 30 h and distilled off the excess of HCOOH. After leaving the residue at –5°C for 24 h, it was diluted with EtOH and filtered; compound **1** was obtained in only 10% yield. Chipen et al. have also tried to synthesize compound **1** from monothiourazole **5** by adding it to a mixture containing H₂O, HNO₃, and NaNO₂ and maintaining the temperature 35–40°C. After cooling the

solution, a white precipitate of the corresponding disulfide was obtained which was removed by filtration, and the filtrate was neutralized with NaOAc, evaporated to dryness and extracted thrice with EtOH. The alcoholic part was evaporated yielding only 3.3% of product **1**.³⁴ Kröger et al. synthesized, by heating carbohydrazine with ethyl orthoformate in a water bath for 3 h, 4-amino-1*H*-1,2,4-triazol-5(4*H*)-one (**6**) in 70% yield which upon deamination (diazotization followed by nitrogen removal under heating) produced 1,2,4-triazol-5-one (**1**) in 60% yield.⁴⁹ Compound **1** was also produced by mixing hydrazodicarbonamide with HCOOH under reflux.⁵⁰

1.2. Nitration of 1,2,4-triazol-5-one

Manchot and Noll synthesized NTO by nitrating 1,2,4-triazol-5-one (**1**) with fuming HNO₃ and obtained white solid which becomes yellow, then brown, and decomposes with rapid heating.³³ Chipen et al. nitrated compound **1** with various nitrating mixtures made of fuming HNO₃ and H₂O to obtain yields of NTO between 43.4 and 67.5% (Table 1). They found that the product did not melt, but rather decomposed at 265–268°C.³⁴ They observed that the use of fuming HNO₃ without water resulted in the complete carbonization of TO.³⁴ Several scientists employed similar method for synthesizing NTO. 1,2,4-Triazol-5-one (**1**) was added to fuming or 70% HNO₃ in 3-necked flask and maintaining the temperature of the solution between 0–5°C,

Table 1. Preparation of NTO by nitration of 1,2,4-triazol-5-one (**1**) using different nitrating agents

Compound 1 , g	Nitrating agent		Time required, min	Tempera- ture, °C	Yield of NTO, %	Reference
	Fuming HNO ₃ , ml	H ₂ O, ml				
4.00	4	–	2–4	–*	–**	34
4.00	2	2			–**	
4.00	5	3			50.0	
4.00	6	3			57.2	
10.0	15	8			67.5	
4.00	6	4			43.4	
0.50	70% HNO ₃ (5 ml) under microwave heating (210 W)		10	65	74	37
150	70% HNO ₃ (900 ml)		–	60–70	80	35
0.50	Concd H ₂ SO ₄ (20 ml), NaNO ₃ (0.0074 mol)		120	45–50	68	38
	Concd H ₂ SO ₄ (20 ml), KNO ₃ (0.0074 mol)		120	45–50	70	
	Concd H ₂ SO ₄ (20 ml), AgNO ₃ (0.0074 mol)		120	45–50	79	
0.17	CDN (1 mmol), 96% H ₂ SO ₄ (3 ml), H ₂ O (1 ml)		180	60–65	88	39
	CDN (0.8 mmol), 6% H ₂ SO ₄ (3 ml), H ₂ O (1 ml)				70	
	CDN (0.6 mmol), 96% H ₂ SO ₄ (3 ml), H ₂ O (1 ml)				68	
	CDN (0.4 mmol), 96% H ₂ SO ₄ (3 ml), H ₂ O (1 ml)				66	
	CDN (0.2 mmol), 96% H ₂ SO ₄ (3 ml), H ₂ O (1 ml)				53	

* The reaction mixture was heated up until the start of reaction was visible by intense emission of nitrogen oxides.

** Product carbonizes under these experimental conditions.

and after that the mixture was heated between 30–75°C under refluxed conditions. Depending on the temperature and concentration of the reagents, time taken for the formation of NTO precipitate varied. Thereafter, the obtained NTO was filtered, dried, and recrystallized.^{20,33–35}

NTO can also be synthesized using a different nitrating system (concentrated HNO₃ in a mixture with concentrated H₂SO₄).⁴² Deshmukh et al. employed a nitrating system of cyclodextrin nitrate (CDN) – H₂SO₄, in which the use of solid CDN allowed for a safer handling than HNO₃. A 88% yield of NTO was obtained when the ratio of 1,2,4-triazol-5-one (**1**) to CDN was 2:1. H₂SO₄ was added to CDN under cooling conditions, and after 1 h of stirring and addition of H₂O, compound **1** was added to the mixture. The round-bottom flask was heated maintaining the temperature at 60–65°C for 2 h and followed by cooling. The resulting NTO was extracted with EtOAc and purified using column chromatography employing *n*-hexane–EtOAc, 4:1, as eluent.³⁹

Saikia et al. used metal nitrates (NaNO₃, KNO₃, or AgNO₃) and H₂SO₄ as a nitrating system at reflux and noticed that the yield was higher when AgNO₃ was used followed by KNO₃ and NaNO₃.³⁸ In the methods discussed above, a conventional heating source was used which required more time to produce the nitration product and some of the product was lost as a result of degradation. To avoid such issues, a microwave was employed as a heating source. The time taken for microwave synthesis was only 10 min in contrast to conventional technique that required 120 min.³⁷ The yield of NTO obtained by employing two-step synthesis involving (i) synthesis of TO followed by (ii) nitration of compound **1** to produce NTO using different nitration conditions is presented in Table 1.

The obtained yield of NTO is affected by varying the molar ratio, concentration, time, temperature, and type of nitrating system taken. It is well known that the standard temperature used for the nitration of NTO is 60–65°C.³⁹ Spear et al. reported a one-pot synthesis of NTO from semicarbazide hydrochloride (**3**·HCl) and HCOOH using a mixture of concentrated H₂SO₄ and HNO₃ as the nitrating system (Table 2) and observed a decrease in the yield of NTO as the reaction time was increased under identical

conditions and the reaction was more vigorous when this acid mixture was used as compared to that when solely concentrated HNO₃ (69.9% yield) was used for the nitration.⁴⁰

Zbarsky and Yudin⁵¹ conducted a thorough investigation of the kinetics of nitration of 1,2,4-triazol-5-one (**1**) using 70–100% HNO₃. Because the activation energy of *N*-nitro-1,2,4-triazol-5-one destruction in 100% HNO₃ is larger than the activation energy of 1,2,4-triazol-5-one (**1**) nitration, the NTO yield decreases as the reaction temperature rises. Instead, rapid *N*-nitro-1,2,4-triazol-5-one formation occurs during the nitration of 1,2,4-triazol-5-one (**1**) in concentrated HNO₃. This has a substantial impact on the NTO synthesis process and results in a considerable drop in the yield of NTO produced. The yield of NTO was independent of both the initial acid concentration in the range of 90–98% HNO₃ concentration and the excess range of 4–8 equiv HNO₃ with respect to compound **1** at temperatures 273–303K, and the reaction time decreased with increasing the temperature. It was also found that when the HNO₃ excess over compound **1** was increased, the yield in 98% HNO₃ declined dramatically.^{51,52} It has been observed that a range of thermal phenomena can affect the process of nitration at varying concentration of HNO₃. The safety of NTO manufacture may be ensured by a better knowledge of such heat effects.²

Zbarsky et al.⁵³ investigated kinetics of the nitration of 1,2,4-triazol-5-one (**1**) in HNO₃/H₂SO₄ mixture using 60–93% H₂SO₄ and determined that at 93% H₂SO₄, NTO starts to slowly decompose due to its interaction with the acid mixture. Therefore, the concentration of NTO drops from 94 ± 3 to 18 ± 5% with increasing concentration of H₂SO₄ from 63–78 to 93%. The nitration of compound **1** in the acid mixture was found to follow the first-order reaction kinetics.⁵³ Trzciński et al.⁵⁴ used calorimetric measurements to investigate the heat and kinetics of reactions, as well as modeling the events that occur in a nitration process of compound **1**. The authors calculated the average heat of reaction using several HNO₃–H₂SO₄–H₂O mixtures. The total heat of the nitration reaction is composed of the thermal effects of dissolution and nitration.⁵⁴ A detailed investigation of heat effects of NTO synthesis in HNO₃ was carried out by Zhao et al.⁵⁵ They measured the heat of five thermal effects during NTO synthesis: the heat of nitration reaction, the heat of crystallization of NTO, the heat of dissolution of compound **1**, as well as the heat effects of process of dosing compound **1** and changing the concentration of HNO₃.⁵⁵ The authors observed that during synthesis operations with 66–96% HNO₃, the heat of reaction was the primary contributor to the overall exothermic effect; the contribution ability rank of the other four thermal effects changed depending on the HNO₃ concentration used.⁵⁵

Table 2. One-pot synthesis of NTO using acid mixture for the nitration⁴⁰

The reaction scheme shows the conversion of 3·HCl and HCOOH to compound **1** (1,2,4-triazol-5-one) with the loss of HCl. Compound **1** is then nitrated using HNO₃ and H₂SO₄ at 65°C to produce NTO (N-nitro-1,2,4-triazol-5-one).

3·HCl, g	HCOOH, ml	Concd HNO ₃ , ml	Concd H ₂ SO ₄ , ml	Time, min	Yield of NTO, %*
33.45	34.5	125	20	90	77.0
33.45	34.5	125	20	135	73.4
33.45	34.5	100	20	100	77.4
33.45	34.5	100	10	150	72.3
133.8	138.0	500	80	480	56.3
33.45	34.5	75	0	90	69.9

* Calculated over 2 steps with respect to compound **3**·HCl.

2. IMPROVING PARTICLE MORPHOLOGY AND REDUCING SIZE

The morphology and size of the NTO particles can vary, and it is necessary for processing to obtain NTO particles of the correct morphology and appropriate size. A variety

of recrystallization solvents can be employed to change its morphology. The particle size of the synthesized NTO can be reduced depending upon the method used.^{40,44–46} When the size of energetic materials is reduced to the nanometer scale, their physical and chemical properties change drastically.⁵⁶

2.1. Morphology

When recrystallizing from H₂O, the obtained NTO particles are jagged rod-like and tend to agglomerate. NTO crystals obtained by recrystallization from low molecular weight alcohols are spherical and hence are more preferred compared to rod-like crystals.⁴¹ Recrystallization of bulk NTO from DMSO and CH₂Cl₂ produces finely divided NTO particles with uniform size. Briefly, NTO particles were dissolved in DMSO at 70°C followed by diluting this NTO–DMSO mixture with CH₂Cl₂ and passing the resulting solution through an injector/needle with internal diameter of 0.70 mm to 0.40 mm. By filtration and drying, NTO particles were produced with the increased surface area from 2702 to 56742 cm²/cm³. Particles with larger surface area can be obtained when the stream of atomized NTO/DMSO in inert gas is added into the CH₂Cl₂ solvent.⁴³

Lee et al.⁴² conducted a study on the effect of ultrasound on the recrystallization of NTO from H₂O by varying the sonication time, stirring speed, and ultrasound frequency. Crystals obtained by the conventional method (dissolving NTO in a solvent at a higher temperature using traditional

heating on a hot plate or a burner, then lowering the temperature in an ice bath to obtain crystals) were hexagonal or cubic with a broad particle size distribution. However, NTO recrystallized using a 28 kHz sonicator was orthorhombic and of a narrower particle size distribution (10–20 μm). However, when a 47 kHz sonicator was used, the particles were cubical and the particle size distribution was broad (40–60 μm). Increasing the sonication time broadens the particle size distribution as shown in images (Fig. 2) obtained using scanning electron microscopy (SEM).⁴² To compare the morphology of NTO particles produced by sonocrystallization (Fig. 2, a–d),⁴² also the images of nanosize NTO (Fig. 2, e), and spherical NTO (Fig. 2, f), obtained by cooling crystallization in a H₂O and *N*-methylpyrrolidine (NMP) cosolvent mixture, are shown.

Kim and Kim obtained spherical NTO crystals by varying the ratio of cosolvents (NMP) and H₂O as well as changing the agitation time. They concluded that the spherical morphology of NTO crystals increases as the cooling rate and NMP content increased.⁵⁷

2.2. NTO nanoparticles

Nanosizing of the energetic materials results in decreased decomposition temperature and increased burn rate. Reduction in the particle size of energetic materials can be achieved using top-down or bottom-up techniques like freeze drying, sol–gel, grinding, wet milling, electrospray crystallization, and evaporation crystallization among others.^{56,58,59} It is well known that reducing the size

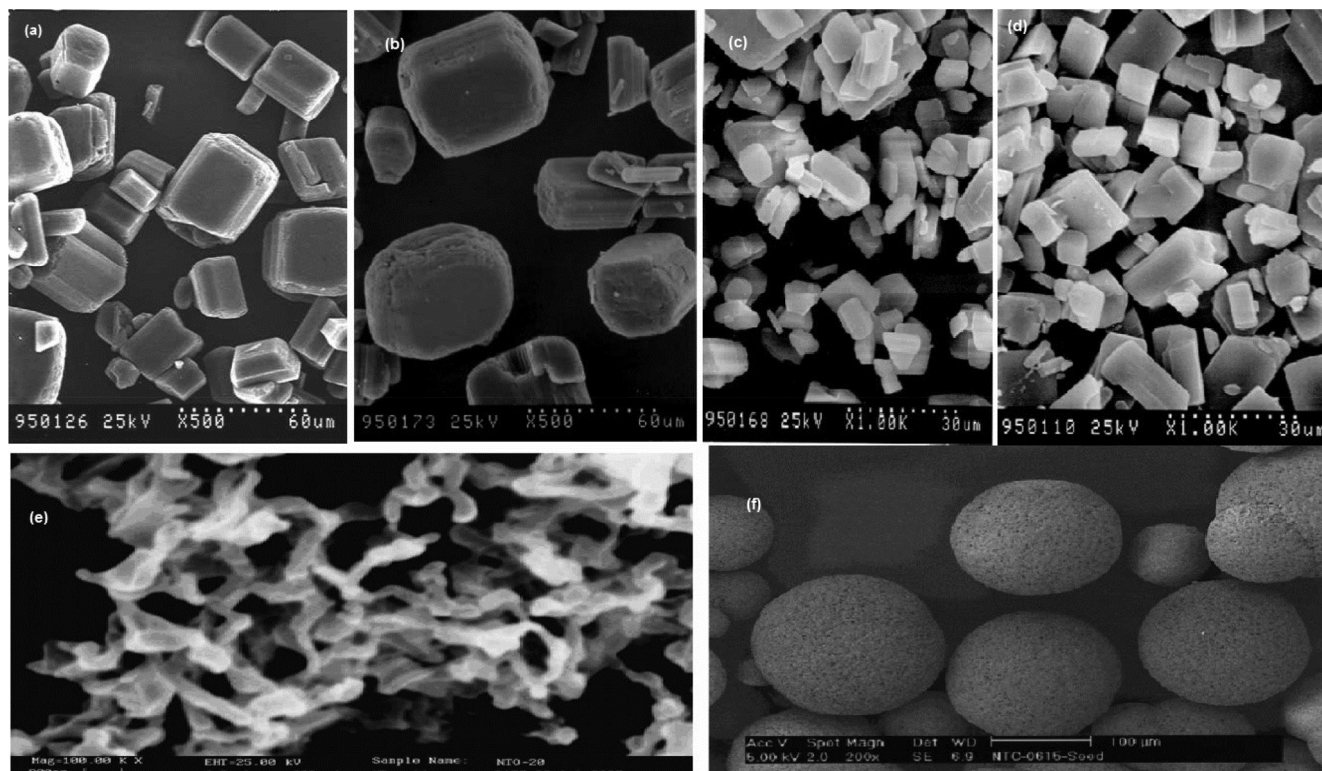


Figure 2. SEM images of NTO particles, obtained by sonocrystallization at given ultrasound frequency and stirring speed, shown in specified magnification, respectively: (a) 47 kHz, 200 rpm, 500×; (b) 47 kHz, 600 rpm, 500×; (c) 28 kHz, 200 rpm, 1000×; (d) 28 kHz, 400 rpm, 1000× (reproduced with permission);⁴² (e) Nano-NTO, magnification 10⁵× (reproduced with permission);⁴⁴ (f) spherical NTO crystal in H₂O–NMP cosolvent system at cooling rate of 10K/min, magnification 200× (reproduced with permission).⁵⁷

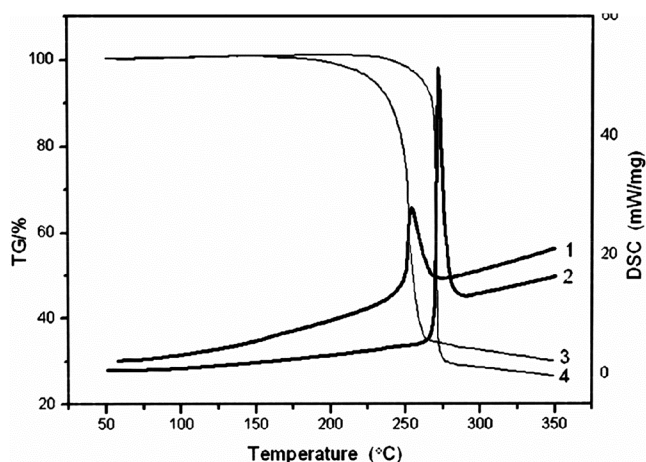


Figure 3. DSC curves of (1) nano-NTO and (2) micro-NTO; TGA curves of (3) nano-NTO and (4) micro-NTO (reprinted with permission).⁴⁴

of the NTO particles increases the surface area and decreases the decomposition temperature. Yang et al. produced NTO nanoparticles (nano-NTO) by using the method of spray freezing into liquid consisting of spraying an aqueous feed of NTO into cryogenic liquid nitrogen. The obtained nanoparticles had an elongated shape in 70–90 nm width and 200–300 nm length. The comparison of the results of differential scanning calorimetry (DSC) and thermogravimetric (TG) analysis of micron-sized and nanosized NTO showed that nano-NTO decomposes at a lower temperature compared to its micron-sized counterpart (micro-NTO) (Fig. 3). In the DSC analysis the exothermic peak corresponding to nano-NTO was 16°C lower than that of micro-NTO and similarly the TG analysis showed that nano-NTO decomposes at a lower temperature than micro-NTO. DSC and TG thermograms are given in Figure 3.⁴⁴ Nanosized NTO with a particle size of 10–30 nm can be obtained by the water-in-oil reverse microemulsion technique using liquid paraffin as the oil phase, polyoxyethylene sorbitan monooleate (or Polysorbate-80, Tween 80)/sorbitan monolaurate (span 80) as surfactants, and normal alcohols like *n*-butanol, *n*-pentanol, *n*-hexanol, and *n*-heptanol as a cosurfactant.²

2.3. Submicron NTO

Submicron-sized NTO was produced by preparing a solution of NTO in THF and pouring this solution into chilled *n*-hexane at 0°C with vigorous stirring followed by filtration and drying. Similarly, an NTO/Al nanocomposite was prepared by dispersing 15% nanosized Al powder of 40 nm particle size into a solution of NTO in THF followed by pouring it into a cooled *n*-hexane solution. The obtained precipitates were filtered and dried in an oven. The size of the obtained NTO was 300 nm.⁴⁵

3. CHARACTERIZATION OF NTO

NTO is white crystalline solid which does not melt, but instead decomposes at 265–268°C and is acidic (pH 2.85 for a 0.1 M aqueous solution) in nature and hence it tends to form various salts with metals.³⁴ NTO forms a yellow

Table 3. Solubility of NTO in representative solvents⁴⁰

Solvent	Temperature, °C	Solubility, g/100 ml
H ₂ O	4.85	0.72
	18.95	1.28
	43.3	2.6
	100	~10
Me ₂ CO	18.95	1.68
EtOAc	18.95	0.28
CH ₂ Cl ₂	18.95	<0.02

aqueous solution.²⁰ Solubility of NTO in Me₂CO, H₂O, EtOAc, and CH₂Cl₂ is presented in Table 3. NTO is well soluble in H₂O, dimethyl formate, TFA, MeCN, dioxane, and DMSO. NTO is partially soluble in solvents like EtOAc, CHCl₃, PhMe, Et₂O and insoluble in CH₂Cl₂.⁴⁰ Physical and chemical properties of NTO are represented in Table 4.

Table 4. Properties of NTO

Sr. No.	Property	Data	References
1	Empirical formula	C ₂ H ₂ N ₄ O ₃	20
2	Mass spectrum, <i>m/z</i>	130 [M] ⁺	52
3	Decomposition temperature	273°C	46
4	Crystal polymorphs	Two forms (α and β form)	60
5	Density, g·cm ⁻³	1.93	20
		1.84	35
		1.68–1.70	45
6	pK _a	3.67	20
7	UV-Vis spectrum, λ_{\max} (varies with pH)	0.01 M aqueous solution: 315 nm, 325 nm	39, 46, 61
9	IR spectrum, ν , cm ⁻¹	3196 (NH), 1689 (C=O), 1540 and 1336 (–NO ₂) in KBr	37
10	¹ H NMR spectrum (DMSO- <i>d</i> ₆), δ , ppm	8.28 (2H, br. s, 2NH)	37
	¹³ C NMR spectrum (DMSO- <i>d</i> ₆), δ , ppm	148.0 (CNO ₂); 154.4 (C=O)	20
12	DTA exotherm, °C	>236, 264	20, 35
13	DSC, T max/°C	256 (Exo.), 257	37, 38
14	Impact sensitivity, cm	>280	20
		87	35
		>320	45
15	Vacuum stability, ml	0.49 (120°C, 48 h)	35
16	Velocity of detonation, m/s	7992	35
17	Friction sensitivity, kg	>36	35, 45

3.1. Polymorphism of NTO

NTO has two polymorphs namely α -NTO and β -NTO. Among these two, α -NTO has been found to be more stable. β -NTO is unstable and decomposes within 6 months. Cooling of a hot solution of NTO in various solvents results in long needle-shaped particles of α -NTO. Recrystallization from MeOH or an EtOH–CH₂Cl₂ solution results in the formation of β -NTO. Cutting an α -NTO

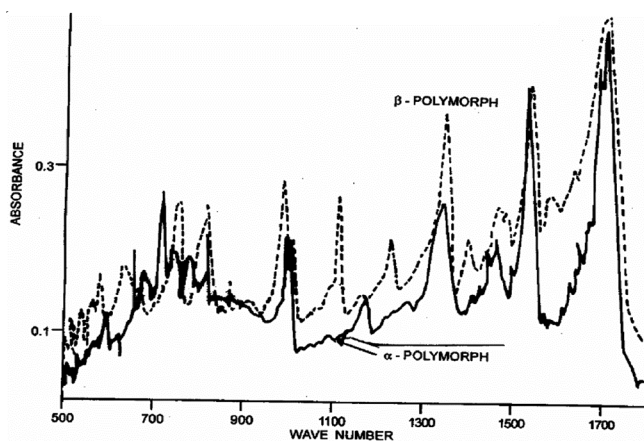


Figure 4. IR spectrum of two polymorphs of NTO (Creative Commons licence).³⁵

needle crystal perpendicularly to the long axis causes the crystal to shatter parallel to that axis. The α - and β -forms of NTO can be distinguished by using various techniques. They exhibit different X-ray diffraction (XRD) patterns, and their IR spectra, too, show differences (Fig. 4). SEM indicates that the particles of β -form tend to agglomerate. Hence, α - and β -NTO can be distinguished using XRD, IR, or SEM.⁶⁰

4. DECOMPOSITION OF NTO

Various techniques have been employed to establish the correct mechanism of decomposition of energetic materials like thermoanalytical techniques, mass spectroscopy, UV irradiation and laser irradiation,^{62–65} and among those techniques TG-FTIR and TG-MS are the most efficient.⁴⁷ Many studies have been carried out to propose the decomposition mechanism of NTO, but its details are still debatable. Although it is believed that the initial step of the decomposition process involves either homolytic cleavage of the C–NO₂ bond or hydrogen abstraction leading to the elimination of HONO molecule.

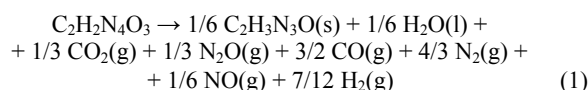
Beard and Sharma exposed NTO and three other explosives (HMX, RDX, and 2,4,6-triamino-1,3,5-trinitrobenzene (TATB)) to X-ray and UV radiation to understand their photochemical sensitivity. The authors observed that the order of radiation damage was RDX > HMX > NTO > TATB, indicating that NTO is more stable to X-ray and UV radiation damage than RDX and HMX. X-ray photoelectron spectroscopy study of radiation-damaged NTO lead to a suggestion that the decomposition of NTO may occur *via* alternative pathways such as loss of NO₂ molecule producing 1,2,4-triazol-5-one (**1**), reduction of the nitro group yielding nitroso-1,2,4-triazol-5-one, and the loss of NO molecule producing urazole.⁶⁶

From a laser-induced mass spectrometry study on the thermal decomposition of NTO, Östmark et al.⁶² proposed that the decomposition of NTO may involve the elimination of the NO₂ group along with a H atom followed by the fragmentation of the azole ring, as the mass spectra consisted of an ion with m/z 83 which is the mass of a fragment resulting from NTO eliminating a HONO molecule. Therefore, it was suggested that HONO elimina-

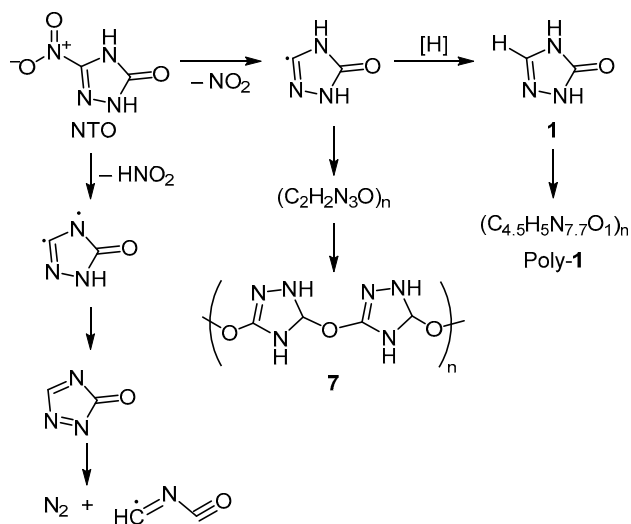
tion could be one possible explanation of the decomposition process. The fragments of m/z 41–44 were ascribed to the azole ring fragmentation.⁶²

Menapace et al. studied the decomposition of NTO by EPR and HPLC techniques under thermal decomposition at 240°C, as well as photochemical decomposition by irradiating a sample with UV. The studies indicated that the decomposition of deuterated NTO (NTO-*d*₂) involves H abstraction from one NTO molecule along with the N–H bond rupture with elimination of NO₂ from another NTO molecule, indicating an intermolecular decomposition mechanism.⁶⁷

Rothgery et al.⁶⁸ carried out the thermal decomposition study of NTO using DSC, TGA-MS, and accelerating rate calorimetry (ARC). They observed that in the DSC analysis no endothermic peak corresponding to melting of NTO was obtained indicating that NTO decomposes without melting. An exothermic peak at 270°C was obtained, and it was also the decomposition temperature obtained by TGA analysis. The residue left at the end of the TGA run had the empirical molecular formula C₂H₃N₃O, but it was not 1,2,4-triazol-5-one (**1**). IR spectroscopy determined that the gases evolved during the TGA decomposition were H₂O, NO, CO₂, CO, and N₂O, but no NO₂ was present at this stage. After some time, a peak corresponding to NO₂ was obtained that could be ascribed to the oxidation of NO. From the ARC study, the adiabatic temperature rise resulted in a heat released of –77 kcal/mol, indicating the total combustion of the sample to CO₂, H₂O, and N₂. It was also concluded that NTO is thermodynamically unstable, but kinetically stable, as high temperature was required to initiate the decomposition. Based on their study, Rothgery et al.⁶⁸ proposed the following summary chemical equation (1) for the stoichiometry of decomposition products of NTO:



The thermal decomposition study of Oxley et al.⁶³ by GC-MS also agreed with the previous studies that H abstraction is an essential part of the decomposition mechanism, as the decomposition of deuterated NTO was slower as compared to proteo-NTO (NTO containing ¹H isotope). They observed that the thermal decomposition of NTO produced CO, CO₂, NO, N₂, and N₂O along with a polymeric residue **7** with an elemental ratio of C₂H₂N₃O. This residue was not of polymeric 1,2,4-triazol-5-one (poly-**1**), as the element ratio in polymeric 1,2,4-triazol-5-one was C_{4.5}H₅N_{7.7}O₁. Decomposition of other compounds containing a triazole ring between 220–280°C was studied, and it was observed that the decomposition of the triazole ring containing a carbonyl or amine group along with the nitro group was higher as compared to the other substituted triazole rings, indicating that there must be some interaction between the carbonyl and NO₂ group that facilitates H abstraction and therefore, the decomposition. The proposed mechanism is depicted in Scheme 3.⁶³ Later on, the same group supported their proposed mechanism by thermolysis of N¹⁵-labelled NTO.⁶⁵

Scheme 3. Proposed mechanism for the decomposition of NTO⁶³

Pressure-dependent IR spectroscopy of NTO decomposition products carried out by Williams et al.⁶⁹ showed that upon heating NTO to 450°C, no measurable quantities of NO₂ or HONO were produced as predicted by the previous studies, but a peak corresponding to NO was present below 1 atm. However, when the pressure was increased, a small quantity of NO₂ was observed along with other stable gases like CO₂, N₂O, HCN, CO, and HNCN. Hence, it was predicted that NO₂ elimination is not the primary decomposition mechanism under such conditions.⁶⁹ Prabhakaran et al. also observed similar gaseous products CO₂, CO, HCN, N₂O, NO, and NO₂ by thermolysis of NTO.⁷⁰ Research of Galante et al. is also in agreement with other similar studies as the thermal decomposition products of NTO determined by GC-MS consisted of CO, CO₂, N₂, N₂O, and HCN.²²

Beardall et al. employed pulsed infrared laser pyrolysis and FT-IR spectroscopy (Fig. 5) and noticed that a peak in the infrared region corresponding to CO₂ was present, which was in agreement with previous work, but peaks corresponding to NO₂ and HONO were absent, and also the decomposition reaction was unimolecular. They proposed that initial ring opening should have taken place by cleavage of the C–N bond between the C atom of the carbonyl group and the adjacent nitrogen. The interaction between the carbonyl group and NO₂ of the same molecule leads to formation of CO₂.^{64,71}

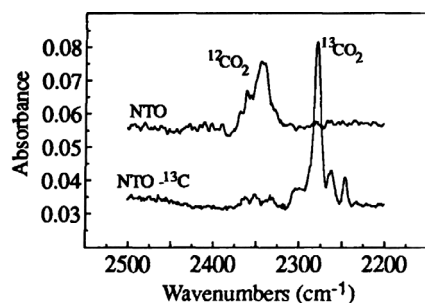


Figure 5. IR spectrum of laser pyrolysis decomposition products of NTO.⁷¹ (Reprinted with permission. Copyright 1996. American Chemical Society.)

Recently, Jiang et al.²¹ employed photoionization mass spectrometry along with molecular dynamics (MD) simulations to investigate the thermal decomposition mechanism of NTO. According to the experimental data and MD simulations, the main products of NTO thermolysis are N₂, CO₂, H₂N₂, NH₃ with some traces of HN₂, H₃N₃, and H₂O.²¹ According to their findings, CONH and CONHCNNH₂ are two important intermediates during the thermal breakdown of NTO. MD simulations support NTO breakdown by direct ring opening in accordance with previous study.⁶⁷ In multimolecular system, in addition to ring opening some molecules undergo H abstraction as well. The findings of the experiments and calculations support the thermal destruction of NTO *via* direct ring opening and intermolecular hydrogen transfer routes. Direct ring opening is the first stage in the breakdown of a single NTO molecule, followed by NO₂ elimination. The residual structure undergoes C–N bond cleavage, resulting in HN₂ dissociation, and the CONCH is eventually broken down into CO and HCN.²¹ Similarly, Lan et al.⁷² proposed the thermal decomposition of NTO based on combined TG-FTIR-MS technique supported by MD simulations. They found that during the thermal decomposition of NTO, C₂HO₃N₄, C₂H₃O₃N₄, C₂N, and NO₂ are the intermediate products, with C₂HO₃N₄ being the most abundant intermediate product. Another study showed that the major gaseous products are H₂O, CO₂, N₂, NH₃, H₂, CH₄, with N₂ being the most abundant.²⁴ Both the recent studies^{21,72} agree in that H abstraction is one of the steps that initiates the thermolysis of NTO.

5. CATALYSTS FOR THE DECOMPOSITION OF NTO

For the better performance of the energetic materials, additives are used in explosive compositions. Some of these catalysts successfully applied to energetic materials are nanometals, like nanometal ferrite, graphene oxide based catalysts, ferrocene-based catalysts, and transition metal oxides.^{70,73–79}

Prabhakaran et al. applied 5% m/m metal oxides as additives to NTO in order to enhance the decomposition of NTO as depicted in Table 5. Based on their study, CuO, PbO, Cu₂O, TiO₂, monobasic lead stearate, Fe₂O₃, ZrO₂, and MgO were found to decrease the decomposition temperature of NTO indicating their catalytic activity for enhancing the thermal decomposition of NTO. On the other hand, additives such as copper chromite (Cu₂Cr₂O₅), CeO₂, NiO, etc., were found to increase the decomposition temperature of NTO indicating that in the presence of these compounds thermal stability of NTO increases.⁷⁰

Hanafi et al. studied the catalytic activity of coordination polymers of triaminoguanidine transition metal (Zn, Co) complexes with graphene oxide (NTO/GO-T-M-T) or without graphene oxide (NTO/T-(Zn, Co)) on NTO (Table 6). The thermal decomposition temperature of NTO without catalyst was 268.7°C, and it was reduced when catalyst was used. T-Zn has a better catalytic activity than T-Co, and GO-T-Zn-T has a better catalytic activity than GO-T-Co-T for enhancing the thermal decomposition of

Table 5. Effect of additives on the thermal decomposition temperature of NTO⁷⁰

Additives	Temperature of decomposition		
	Initial temperature, °C	Maximum temperature, °C	Final temperature, °C
PbO	251	254	273
Cu ₂ O	241	254	273
Monobasic lead stearate	210	255	274
CuO	245	251	273
TiO ₂	229	251	274
ZrO ₂	255	258	286
Fe ₂ O ₃	226	259	268
MgO	190	261	271
No additives	241	262	292
Cu ₂ Cr ₂ O ₅	241	264	295
La ₂ O ₃	264	268	292
Monobasic copper stearate	247	268	291
NiO	262	269	295
CeO ₂	257	271	289
Co ₂ O ₃	210	274	301
ThO ₂	264	276	298

Table 6. Effect of catalysts on thermal decomposition of NTO determined by TGA

Catalyst	Application	Decomposition temperature, °C	Reference
T-Co		255.9	78
T-Zn	Preparing composites of NTO/GO-T-M-T and NTO/T-M	230.9	
GO-T-Co-T		252.4	
GO-T-Zn-T		237.9	
Nano NiO	1% Nanoadditives	–	77
Nano ZnO		–	
Nano Cu	1% Nanoadditive	273	79

NTO. When the same catalyst with 2D-layered graphene oxide was used, it exhibited better catalytic activity for the decomposition of NTO.⁷⁸

Dubey et al. synthesized copper nanoparticles and used them as a catalyst for the thermal decomposition of HMX, NH₄ClO₄, and NTO. The authors found that the decomposition of NH₄ClO₄ was greatly affected in the presence of Cu nanocatalyst, but little catalytic activity of this nanometal was observed for NTO. Moreover, the thermal decomposition of NTO without catalyst was 275°C and that of NTO with 1% nano-Cu additive was 273°C.⁷⁹ Kumar et al. observed that the decomposition temperature of NTO with 1% nano-NiO (crystal size 6 nm) and 1% nano-ZnO (crystal size 31 nm) was decreased compared to that of without nanoadditive. They observed that the catalytic activity of 1% ZnO was better than that of 1% NiO.⁷⁷

6. NTO-BASED ENERGETIC COCRYSTALS

In the domain of HEMs, cocrystallization is still in its early stages of development, but it is already showing signs of promise. Without losing energy output, the cocrystallization technique can increase the overall attributes like

stability, positive oxygen balance, velocity of detonation, thermal performance, etc. The research in the field of the production of energetic cocrystals is increasing, paving the way for novel high EMs with desirable properties.^{2,80} High energetic cocrystals (HECCs) are composed of two or more compounds among which at least one is HEM, attracted by nonbonded interactions.⁸¹ The intramolecular interactions and hydrogen bonds established between the constituents of cocrystals aid in achieving improved characteristics in comparison with their components taken separately.^{2,81}

Azole-based HEMs seems to be of interest for cocrystallization studies, since their molecules have rather excellent hydrogen bond donor or acceptor properties. An example of such an azole derivative is NTO.² Regarding other azoles, Gamekkanda et al.⁹ observed that seven out of nine cocrystal/salts formulations of tetrazole-based energetic materials imparted improved thermal stability in comparison to their individual components. Research in the field of HECC systems containing a less sensitive HEM such as NTO and highly sensitive HEMs have gathered a lot of attention, resulting in experimental as well as theoretical studies.^{9,81–83} Wu et al.⁸⁴ successfully synthesized a HECC consisting of NTO and 5,6,7,8-tetrahydrotetrazolo-[1,5-*b*][1,2,4]triazine (TZTN). The findings revealed that the NTO/TZTN (1:1) cocrystal not only has unique features of its own, but also has the ability to efficiently modify the characteristics of NTO and TZTN. For example, the acidic nature of NTO was neutralized by incorporation of TZTN, and NTO improved the thermal stability of TZTN.

Li et al.⁸⁵ prepared a HECC of HMX/NTO in 1:1 proportion using solvent/antisolvent approach. It was observed that the mechanical sensitivity of the cocrystal has been altered. In comparison to HMX, the typical value of impact sensitivity increases by 14.8 cm, while the explosion percentage of friction sensitivity drops by 40%. The HMX/NTO cocrystals have excellent thermal properties and low sensitivity, resulting in significant benefits in blasting engineering.

Various theoretical studies have been investigated to predict performance and solvent effects on crystal growth of NTO-based cocrystal systems. Liu et al.⁸⁶ carried out quantum chemistry and MD simulations to observe the effects of three solvents (MeOH, EtOAc, and Me₂CO) on NTO/TZTN cocrystal formation and observed that in MeOH, the interaction between the major growth surfaces and the solute molecules (NTO and TZTN) was greater than in other solvents.

Hang et al.⁸⁷ investigated the influence of molar ratios on the explosive performance of hexanitrohexaazaisowurtzitane (CL-20) cocrystals with NTO using MD method. The authors conclude that CL-20/NTO cocrystals with 2:1, 1:1, or 1:2 CL-20/NTO ratio exhibited highest stability as compared to other molar ratios. The CL-20/NTO HECCs exhibited decreased mechanical sensitivity and increased thermal stability indicating improved safety, but the detonation and energetic properties were decreased as compared to CL-20.

Lin et al.⁸⁸ studied crystal system of HMX/NTO using density functional theory methods. The results suggested

that in HMX/NTO HECC system, the intermolecular interactions were governed by CH \cdots O, NH \cdots O, and weak interactions, such as O \cdots O and N \cdots O interactions, and that HMX/NTO cocrystal formation is facilitated at lower temperatures. The detonation velocity and detonation pressure of HMX/NTO cocrystal are 8.73 km/s and 35.14 GPa, respectively, i.e. somewhat lower than those of HMX. The thermal stability criterion of a HEM is met by the HMX/NTO cocrystal. Song et al.⁸³ studied three cocrystal systems of HMX using MD method. The authors concluded that for HMX/NTO, the detonation velocity and pressure rise as the heat of detonation increases. Increasing the amount of HMX in HMX/NTO is advantageous from the standpoint of enhancing detonation velocity and pressure. Similarly, the effect of NTO content on NTO/HMX-based cocrystal system was investigated experimentally.⁸⁹ It was determined that the increasing NTO content in the cocrystal system reduces the mechanical sensitivity and, in restricted areas, improves the thermal safety and decreases the thermal risks of NTO/HMX-based formulations.⁸⁹ For example, NTO/HMX cocrystal based formulation containing 63.7% by wt NTO were less sensitive than the formulation containing 27.3% by wt NTO.⁸⁹

The thermal and photochemical stability of NTO is high compared to its analogous heterocyclic explosives like RDX and HMX with a high performance as a propellant. NTO is less sensitive than other high explosives (HMX, RDX) to external stimuli, and, therefore, it is safer to handle as compared to other high explosives. NTO is a potential substitution for HMX and RDX for propulsion applications. The thermal performance of NTO can be enhanced by adding the catalysts to decrease its thermal decomposition temperature. A general method for the synthesis of NTO was synthesis of 1,2,4-triazol-5-one followed by its nitration. Among the methods for the synthesis of 1,2,4-triazol-5-one, condensing formic acid with semicarbazide hydrochloride is most widely used. The nitration using cyclodextrin nitrate and H₂SO₄ is less hazardous and produced higher yield of NTO compared to the other methods. The standard temperature range for the nitration of 1,2,4-triazol-5-one is 60–70°C. Below 60°C, the nitration is slow and above 70°C, the yield was lowered because of the destruction of the formed product. As the size of the NTO crystal is reduced, its decomposition is enhanced and, hence, nano-NTO decomposes at a lower temperature than micro-NTO. The most accepted path by which decomposition mechanism of NTO proceeds involves either H abstraction or C–NO₂ bond cleavage. NTO is water-soluble and, hence, causes problem of water and soil pollution. The removal of NTO from water streams and soils is, therefore, important. Some metal oxides can enhance the decomposition of NTO, and nanomaterials can be used to enhance the decomposition of NTO for a better performance.

The authors are grateful to Department of Chemistry for providing research facility. RS is also thankful to DST project no SR/NM/NT-1014/2016 (G) for junior research fellowship.

The authors declare that they have no known competing financial interests or personal relationships that could have appeared to influence the work reported in this paper.

References

- Sikder, A. K.; Sikder, N. *J. Hazard. Mater.* **2004**, *112*, 1.
- Hanafi, S.; Trache, D.; Abdous, S.; Bensalem, Z.; Mezroua, A. *Chin. J. Energ. Mater.* **2019**, *27*, 326.
- Fried, L. E.; Manaa, M. R.; Pagoria, P. F.; Simpson, R. L. *Annu. Rev. Mater. Res.* **2001**, *31*, 291.
- Chaturvedi, S.; Dave, P. N. *J. Saudi Chem. Soc.* **2013**, *17*, 135.
- Trache, D.; Tarchoun, A. F. *Crit. Rev. Anal. Chem.* **2019**, *49*, 415.
- Xu, J.-G.; Li, X.-Z.; Wu, H.-F.; Zheng, F.-K.; Chen, J.; Guo, G.-C. *Cryst. Growth Des.* **2019**, *19*, 3934.
- Snyder, C. J.; Wells, L. A.; Chavez, D. E.; Imler, G. H.; Parrish, D. A. *Chem. Commun.* **2019**, 2461.
- Wang, Q.; Shao, Y.; Lu, M. *Chem. Commun.* **2019**, 6062.
- Gamekkanda, J. C.; Sinha, A. S.; Aakeröy, C. B. *Cryst. Growth Des.* **2020**, *20*, 2432.
- Xu, J.; Zheng, S.; Huang, S.; Tian, Y.; Liu, Y.; Zhang, H.; Sun, J. *Chem. Commun.* **2019**, 909.
- Tarchoun, A. F.; Trache, D.; Klapötke, T. M.; Khimeche, K. *Chem. Eng. J.* **2020**, *400*, 125960.
- Li, X.; Hu, S.; Cao, X.; Hu, L.; Deng, P.; Xie, Z. *J. Energ. Mater.* **2020**, *38*, 162.
- Ma, X.; Cai, C.; Sun, W.; Song, W.; Ma, Y.; Liu, X.; Xie, G.; Chen, S.; Gao, S. *ACS Appl. Mater. Interfaces* **2019**, *11*, 9233.
- Deng, P.; Ren, H.; Jiao, Q. *Vacuum* **2019**, *169*, 108882.
- Tan, Y.; Yang, Z.; Wang, H.; Li, H.; Nie, F.; Liu, Y.; Yu, Y. *Cryst. Growth Des.* **2019**, *19*, 4476.
- Wang, P.-C.; Xu, Y.-G.; Wang, Q.; Shao, Y.-L.; Lin, Q.-H.; Lu, M. *Sci. China Mater.* **2019**, *62*, 122.
- Bian, C.; Feng, W.; Lei, Q.; Huang, H.; Li, X.; Wang, J.; Li, C.; Xiao, Z. *Dalton Trans.* **2020**, 368.
- Xiong, H.; Yang, H.; Lei, C.; Yang, P.; Hu, W.; Cheng, G. *Dalton Trans.* **2019**, 14705.
- Badgujar, D. M.; Talawar, M. B.; Asthana, S. N.; Mahulikar, P. P. *J. Hazard. Mater.* **2008**, *151*, 289.
- Lee, K.-Y.; Chapman, L. B.; Cobura, M. D. *J. Energ. Mater.* **1987**, *5*, 27.
- Jiang, L.; Fu, X.; Fan, X.; Li, J.; Xie, W.; Zhou, Z.; Zhang, G. *FirePhysChem* **2021**, *1*, 109. DOI: 10.1016/j.fpc.2021.04.00.
- Galante, E. B. F.; Mai, N.; Ladyman, M. K.; Gill, P. P.; Temple, T. J.; Coulon, F. *J. Energ. Mater.* **2021**, *39*, 85.
- Anniyappan, M.; Talawar, M. B.; Sinha, R. K.; Murthy, R. K. *Combust., Explos. Shock Waves* **2020**, *56*, 495.
- Wei, R.; Fei, Z.; Yoosefian, M. *J. Mol. Liq.* **2021**, *336*, 116372.
- Lent, E. M.; Narizzano, A. M.; Koistinen, K. A.; Johnson, M. S. *Regul. Toxicol. Pharmacol.* **2020**, *112*, 104609.
- Madeira, C. L.; Speet, S. A.; Nieto, C. A.; Abrell, L.; Chorover, J.; Sierra-Alvarez, R.; Field, J. A. *Chemosphere* **2017**, *167*, 478.
- Becher, J. B.; Beal, S. A.; Taylor, S.; Dontsova, K.; Wilcox, D. E. *Chemosphere* **2019**, *228*, 418.
- Terracciano, A.; Christodoulatos, C.; Koutsospyros, A.; Zheng, Z.; Su, T.-L.; Smolinski, B.; Arienti, P.; Meng, X. *Chem. Eng. J.* **2018**, *354*, 481.
- Zhang, M.; Li, C.; Gao, H.; Fu, W.; Li, Y.; Tang, L.; Zhou, Z. *J. Mater. Sci.* **2016**, *51*, 10849.
- Yang, G.; Fude, N. *Sci. Technol. Energ. Mater.* **2006**, *67*, 77.
- Jangid, S. K.; Radhakrishnan, S.; Solanki, V. J.; Singh, M. K.; Pandit, G.; Vijayalakshmi, R.; Sinha, R. K. *J. Energ. Mater.* **2019**, *37*, 320.

32. Benhameda, A.; Trache, D. *Appl. Spectrosc. Rev.* **2020**, *55*, 724.
33. Manchot, W.; Noll, R. *Justus Liebigs Ann. Chem.* **1905**, *343*, 1.
34. Chipen, G. I.; Bokalder, R. P.; Grinshtein, V. Ya. *Chem. Heterocycl. Compd.* **1966**, *2*, 79. [*Khim. Geterotsikl. Soedin.* **1966**, 110.]
35. Mukundan, T.; Purandare, G. N.; Nair, J. K.; Pansare, S. M.; Sinha, R. K.; Singh, H. *Def. Sci. J.* **2002**, *52*(2), 127.
36. Ciller Cortes, J. A.; Mendez Perez, A. EP Patent 0585235.
37. Saikia, A.; Sivabalan, R.; Gore, G. M.; Sikder, A. K. *Propellants, Explos., Pyrotech.* **2012**, *37*, 540.
38. Saikia, A.; Sivabalan, R.; Gore, G. M.; Sikder, A. K. *J. Sci. Ind. Res.* **2014**, *73*, 485.
39. Deshmukh, M. B.; Wagh, N. D.; Sikder, A. K.; Borse, A. U.; Dalal, D. S. *Ind. Eng. Chem. Res.* **2014**, *53*, 19375.
40. Spear, R. J.; Louey, C. N.; Wolfson, M. G. *A Preliminary Assessment of 3-Nitro-1,2,4-triazol-5-one (NTO) as an Insensitive High Explosive*; MRL technical report MRL-TR-89-18; DSTO Materials Research Laboratory: Maribyrnong, 1989.
41. Collignon, S. L. US Patent 4894462.
42. Lee, H.-Y.; Koo, K.-K.; Haam, S.; Kim, S.-H.; Kim, H.-S.; Park, B.-S. *J. Chem. Eng. Jpn.* **2000**, *33*, 842.
43. Kayser, E. G. US Statutory Invention Registration H990.
44. Yang, G.; Nie, F.; Li, J.; Guo, Q.; Qiao, Z. *J. Energ. Mater.* **2007**, *25*, 35.
45. Lee, K.-Y.; Asay, B. W.; Kennedy, J. E. US Patent 8557066.
46. Smith, M. W.; Cliff, M. D. *NTO-Based Explosive Formulations: A Technology Review*; Technical report DSTO-TR-0796; DSTO Aeronautical and Maritime Research Laboratory: Salisbury, 1999.
47. Rozin, Y. A.; Belyaev, N. A.; Bakulev, V. A.; Leban, I.; Azev, Y. A. *Chem. Heterocycl. Compd.* **2011**, *46*, 1534. [*Khim. Geterotsikl. Soedin.* **2010**, 1896.]
48. Starodubova, N. V.; Nikitin, V. G.; Kashaev, V. A.; Mezheritsky, S. E.; Makarov, V. V.; Marakhanova, D. A. *Vestn. Kazan. Tekhnol. Univ.* **2017**, *20*(4), 8.
49. Kröger, C.-F.; Hummel, L.; Mutscher, M.; Beyer, H. *Chem. Ber.* **1965**, *98*, 3025.
50. Rothgery, E. F. US Patent 9203424.
51. Zbarsky, V. L.; Yudin, N. V. *Propellants, Explos., Pyrotech.* **2005**, *30*, 298.
52. Viswanath, D. S.; Ghosh, T. K.; Boddu, V. M. *Emerging Energetic Materials: Synthesis, Physicochemical, and Detonation Properties*; Springer: Dordrecht, 2018, p. 163.
53. Zbarsky, V. L.; Yudin, N. V.; Urazow, A. N.; Drachenina, A. In *Proceedings of the 10th Seminar "New Trends in Research of Energetic Materials"*; University of Pardubice: Pardubice, 2007, p. 978.
54. Trzciński, W. A.; Szala, M.; Rejmer, W. *Propellants, Explos., Pyrotech.* **2015**, *40*, 498.
55. Zhao, Y.; Chen, S.; Jin, S.; Li, Z.; Zhang, X.; Wang, L.; Mao, Y.; Guo, H.; Li, L. *J. Therm. Anal. Calorim.* **2017**, *128*, 301.
56. Gao, B.; Qiao, Z.; Yang, G. In *Nanomaterials in Rocket Propulsion Systems*; Yan, Q.-L.; He, G.-Q.; Liu, P.-J.; Gozin, M., Eds.; Elsevier: Amsterdam, 2019, p. 31.
57. Kim, K.-J.; Kim, K.-M. *Powder Technol.* **2002**, *122*, 46.
58. Ma, X.; Li, Y.; Hussain, I.; Shen, R.; Yang, G.; Zhang, K. *Adv. Mater.* **2020**, *32*, 2001291.
59. Trache, D.; DeLuca, L. T. *Nanomaterials* **2020**, *10*, 2347.
60. Lee, K.; Gilardi, R. In *Structure and Properties of Energetic Materials*; Liebenberg, D. H.; Armstrong, R. W.; Gilman, J. J., Eds.; Materials Research Society: Pittsburgh, 1993, p. 237.
61. Wallace, L.; Cronin, M. P.; Day, A. I.; Buck, D. P. *Environ. Sci. Technol.* **2009**, *43*, 1993.
62. Östmark, H.; Bergman, H.; Åqvist, G. *Thermochim. Acta* **1993**, *213*, 165.
63. Oxley, J. C.; Smith, J. L.; Zhou, Z.; McKenney, R. L. *J. Phys. Chem.* **1995**, *99*, 10383.
64. Beardall, D. J.; Botcher, T. R.; Wight, C. A. *MRS Online Proc. Libr.* **1995**, *418*, 379.
65. Oxley, J. C.; Smith, J. L.; Rogers, E.; Dong, X. X. *J. Phys. Chem. A* **1997**, *101*, 3531.
66. Beard, B. C.; Sharma, J. J. *Energ. Mater.* **1989**, *7*, 181.
67. Menapace, J. A.; Marlin, J. E.; Bruss, D. R.; Dascher, R. V. *J. Phys. Chem.* **1991**, *95*, 5509.
68. Rothgery, E. F.; Audette, D. E.; Wedlich, R. C.; Csejka, D. A. *Thermochim. Acta* **1991**, *185*, 235.
69. Williams, G. K.; Palopoli, S. F.; Brill, T. B. *Combust. Flame* **1994**, *98*, 197.
70. Prabhakaran, K. V.; Naidu, S. R.; Kurian, E. M. *Thermochim. Acta* **1994**, *241*, 199.
71. Botcher, T. R.; Beardall, D. J.; Wight, C. A.; Fan, L.; Burkey, T. J. *J. Phys. Chem.* **1996**, *100*, 8802.
72. Lan, G.; Li, J.; Zhang, G.; Ruan, J.; Lu, Z.; Jin, S.; Cao, D.; Wang, J. *Fuel* **2021**, *295*, 120655.
73. Chaturvedi, S.; Dave, P. N. *J. Exp. Nanosci.* **2012**, *7*, 205.
74. Vara, J. A.; Dave, P. N.; Chaturvedi, S. *Def. Technol.* **2019**, *15*, 629.
75. Usman, M.; Wang, L.; Yu, H.; Haq, F.; Haroon, M.; Summe Ullah, R.; Khan, A.; Fahad, S.; Nazir, A.; Elshaarani, T. *J. Organomet. Chem.* **2018**, *872*, 40.
76. Bagalkote, V.; Grinstein, D.; Natan, B. *Propellants, Explos., Pyrotech.* **2018**, *43*, 136.
77. Kumar, D.; Kapoor, I. P. S.; Singh, G.; Siril, P. F.; Tripathi, A. M. *Propellants, Explos., Pyrotech.* **2011**, *36*, 268.
78. Hanafi, S.; Trache, D.; He, W.; Xie, W.-X.; Mezroua, A.; Yan, Q.-L. *Thermochim. Acta* **2020**, *692*, 178747.
79. Dubey, R.; Srivastava, P.; Kapoor, I. P. S.; Singh, G. *Thermochim. Acta* **2012**, *549*, 102.
80. Liu, G.; Wei, S. H.; Zhang, C. *Cryst. Growth Des.* **2020**, *20*, 7065.
81. Zhang, C.; Xue, X.; Cao, Y.; Zhou, J.; Zhang, A.; Li, H.; Zhou, Y.; Xu, R.; Gao, T. *CrystEngComm* **2014**, *16*, 5905.
82. Zhang, L.; Wu, J.-Z.; Jiang, S.-L.; Yu, Y.; Chen, J. *Phys. Chem. Chem. Phys.* **2016**, *18*, 26960.
83. Song, K.; Ren, F.; Zhang, S.; Shi, W. *J. Mol. Model.* **2016**, *22*, 249.
84. Wu, J. T.; Zhang, J. G.; Li, T.; Li, Z. M.; Zhang, T. L. *RSC Adv.* **2015**, *5*, 28354.
85. Li, J. C.; Jiao, Q. J.; Gong, Y. G.; Wang, Y. Y.; Liang, T.; Sun, J. *IOP Conf. Ser.: Mater. Sci. Eng.* **2018**, *292*, 012032.
86. Liu, Y.; Gou, R.; Zhang, S.; Chen, Y.; Cheng, H. J.; Chen, M. *Comput. Mater. Sci.* **2019**, *163*, 308.
87. Hang, G. Y.; Yu, W. L.; Wang, T.; Wang, J.-T.; Li, Z. *Theor. Chem. Acc.* **2018**, *137*, 114.
88. Lin, H.; Zhu, S.-G.; Zhang, L.; Peng, X.-H.; Chen, P.-Y.; Li, H.-Z. *Int. J. Quantum Chem.* **2013**, *113*, 1591.
89. Du, L.; Jin, S.; Shu, Q.; Li, L.; Chen, K.; Chen, M.; Wang, J. *Def. Technol.* **2021**. <https://doi.org/10.1016/j.dt.2021.04.002>